Selective CO_2 hydrogenation reaction using recyclable TiO_2 supported Ruthenium nanoparticles

Praveenkumar R. Upadhyay, Vivek Srivastava*

Basic Sciences: Chemistry, NIIT University, NH-8 Jaipur/Delhi Highway, Neemrana, Rajasthan, 301705, India

*Corresponding author: Tel: (+91)1494302423; E-mail: vivek.shrivastava@niituniversity.in

Received: 06 March 2016, Revised: 19 September 2016 and Accepted: 21 September 2016

DOI: 10.5185/amp.2017/703
www.vbripress.com/amp

Abstract

Stable, well dispersed and agglomeration free Ru metal doped TiO_2 nanoparticles were produced by a sol gel method (with and without ionic liquid reaction medium). Such unique physiochemical properties of Ru-TiO_2-IL catalyst were utilized as catalysts for CO_2 hydrogenation reaction in task specific ionic liquid medium. Low catalysts loading, moisture/air stability, high selectivity, easy catalyst synthesis protocol as well as stress-free reaction condition along with 5 times catalysts recycling are the major outcomes of the proposed report. Copyright © 2017 VBRI Press.

Keywords: CO_2 Hydrogenation, carbon sequestration, formic acid, ruthenium metal, titanium dioxide, nanoparticles.

Introduction

The reduction of CO_2 emission into the atmosphere is an urgent necessity since this gas is considered as the main content for the greenhouse effect. Various physiochemical methods were reported to fix the CO_2 gas, like fixation as carbonates, geological or ocean storage or afforestation **[1,2]** but unfortunately, these approaches have severe drawbacks in terms of economic factors, safety, efficiency, and reliability of their immediate application.

Hydrogenation reaction is one of most important reaction for the synthesis of industrially important chemicals, such as aldehydes, alcohols, esters and acids from cheap and renewable chemical sources **[3-5]**. Many transition metals were counted as an active and promising catalyst for the selective hydrogenation of organic compounds **[4-11]** including CO_2 hydrogenation reaction. In various reports Ru, Pd, Pt, Rh, and Zn metal were supported on organic-inorganic supports (polymeric, ionic liquids, silica, clay, zeolite etc) for different hydrogenation reactions. Regrettably, in most of the reports, these catalytic systems suffer with the tedious catalyst synthesis procedure, high catalyst loading and catalyst leaching during recycling experiments **[12, 13]**. In recent years, nanoparticles have attracted a significant interest due to their impending applications in a variety of organic transformations and hydrogenation is one of them **[13-15]**. To attain optimal dispersion and to quash aggregation of active phases, metal nanoparticles were commonly supported on the surface of solid career **[12-20]**.

In this approach, TiO_2 was used as a support to accommodate Ru metal nanoparticles, as TiO_2 offers wide chemical stability and a non-stoichiometric phase. TiO_2 also provides as a good acidic support and its anatase phase delivers a better surface area in order to attain good catalytic properties **[21-25]**. In this report, we also extended the application of ionic liquid as an active reaction medium not only for the synthesis of catalysts but also to perform the hydrogenation reaction. As per the strategy, we used NR2 (R= CH_3) containing imidazolium based ionic liquids as reaction medium for ruthenium metal doped TiO_2 nanoparticles catalyzed hydrogenation reaction of CO_2 **[20-25]**. Ionic liquid containing amino groups were expected to capture partial CO_2 hydrogenated products and thus control the selectivity of this reaction with added advantages of easy product isolation and catalysts recycling.

Experimental

Materials

Reagent Plus® grade ruthenium (III) chloride hydrate (98.5%) and titanium tetra isopropoxide (98.5%) were purchased from Aldrich. Other ReagentPlus® and extra pure grade chemicals were purchased from spectrochem. Nuclear Magnetic Resonance (NMR) spectra were recorded on a standard Bruker 300WB spectrometer with an Avance console at 400 and 100 MHz for 1H NMR. All the hydrogenation reactions were carried out in a 100mL stainless steel autoclave (Amar Equipment, India). The catalyst material was characterized by TEM

(Hitachi S-3700N) and Energy-dispersive X-ray spectroscopy (EDX) (Perkin Elmer, PHI 1600 spectrometer). FTIR data for all the samples were studied with Bruker Tensor-27. 1, 3-di (N, N-dimethylaminoethyl)-2-methylimidazolium nonafluoro-butanesulfonate ([DAMI][$CF_3CF_2CF_2CF_2SO_3$]), 1, 3-di (N, N-dimethylaminoethyl)-2-methylimidazolium tetrafluoroborate ([DAMI][BF_4)] and 1-butyl-3-methylimidazolium chloride ionic liquids were synthesized as per reported procedure **[25]**. FTIR data for all the samples were studied with Bruker Tensor-27. The morphology of catalysts was investigated by transmission electron microscopy (TEM) using a Philips CM12 instrument. XRD was performed on Philips X-Pert diffractometer. The normalized X-ray absorption near stretcher (XANES) spectra was recorded on BL01C1.

Catalysts preparation

The precursor solution was prepared by adding titanium tetra isopropoxide (TTIP, 98%) in the glacial acetic acid (GAA, 98%), followed by addition of DM water (DMW). The molar ratio of TTP: GAA: DMW must be kept at 1:10:250. The resulting mass was stirred at 45^{o}C for 2 hours later, 10 mL of 1M $RuCl_3$. $3H_2O$ was added and the complete reaction mass was stirred for next 5 hours at 80^{o}C. Centrifugation technique was used for purification and isolation of the resulting material. The material was tried under reduced pressure for the next 3 h at 40^{o}C to obtain Ru-TiO_2.

In the synthesis of Ru-TiO_2-IL catalyst, while preparing the precursor solution, [bmim][BF_4] was added along with other materials in the following molar ratio [bimim][BF_4]: TTP: DMW=0. 5: 1:250.

Synthesis of monoamine/diamine functionalized ionic liquids

The 250 mL, single neck round bottom flask was charged with methanol (100mL), NaOH (1.1 equiv) and 1-(N, N-dimethylaminoethyl)-2, 3- dimethylimidazolium bromide hydrobromide or, 3-di(N,N-dimethylaminoethyl)-2-methylimidazolium bromide dihydrobromide (1 equiv) **[25]**. The total reaction mixture was allowed to stir for 1 hour at room temperature (25-30^{o}C). 50% aqueous solution of sodium tetrafluoroborate or lithium *bis* (trifluoromethylsulfonyl) imide or Lithium nonafluorobutanesulfonate (1.1 equiv) was then added and the mixture stirred for 2 hours at room temperature. After removing the water, dichloromethane (3 x 5mL ml) was used to recover the reaction product. The solid NaBr was removed by simple filtration.

[DAMI][$CF_3CF_2CF_2CF_2SO_3$]

1H NMR (400 MHz, MeOD): d=2.58 (s, 12H), 2.82 (s, 3H), 2.88 (t, 4H), 4.47 (s, 4H), 7.72 ppm (d, 2H). Positive ion HRMS (EI) m/z found: 313.1663 (calculated for $C_{12}H_{26}BF_4N_4$, M+ requires: 313.2181).

[DAMI] [BF_4]

1H NMR (400 MHz, CDCl3): d=2.48 (s, 12H), 2.79 (s, 3H), 2.85 (t, 4H), 4.43 (s, 4H), 7.71 ppm (d, 2H). Positive ion HRMS (EI) m/z found: 525.1541 (calculated for $C_{16}H_{26}F_9O_3S$, M+ requires: 525.1580).

Hydrogenation reaction

The high-pressure autoclave (100 mL) was charged with catalysts, ionic liquid and water (2mL). Then the oxygen of reaction vessel was replaced by CO_2 /H_2 gas. Reaction mass was allowed to stir for 2.5 hours at 100^{o}C. Later the reaction vessel was allowed to cool (2-5^{o}C) with the help of cold water. A small amount of crude reaction mass was used for ^{1}HNMR analysis. Water was evaporated carefully from the reaction mass at 50^{o}C under vacuum, then formic acid was isolated from the reaction mass with the help of nitrogen gas flow at 75-80^{o}C, passing through the water trap, in order to capture formic acid. Acid base titration was used to calculate the amount formic acid in water trap. The results obtained from ^{1}HNMR analysis as well as from titration method were in full agreement with each other.

After isolating, the catalytic system from reaction mass, it was washed with ether (5 x2mL) and dried under reduced pressure for the next 1 hour. Then the catalytic system went for the next recycling run and all the steps were completed as per above mentioned CO_2 hydrogenation procedure.

Results and discussion

We synthesized two different ruthenium metal doped TiO_2 nanoparticles with and without ionic liquids, named as Ru-TiO_2-IL and Ru-TiO_2 respectively, followed by sol-gel method and calcined over 250^{o}C for 5 hours. The XRD pattern of TiO_2 was compared with Ru-TiO_2-IL and Ru-TiO_2 **Fig. 1** from the wide angle XRD pattern, the titania samples were found only in anatase phase with their characteristic diffraction peaks of 2degree values near 42- 44^o, assigned to metallic ruthenium (PDF no. 06-0633) were observed for Ru-TiO_2 catalyst [**26-27]**. However, there were no characteristic peaks of Ru^o observed on the Ru-TiO_2-IL catalyst, indicating a high dispersion of Ru on the TiO_2 support.

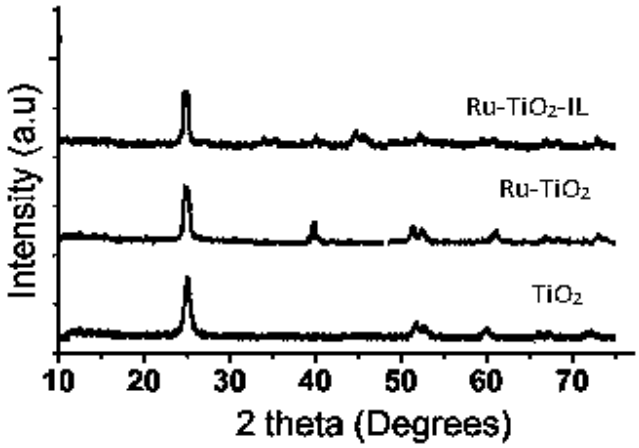

Fig. 1. XRD data for Ruthenium metal doped Titanium dioxide nanoparticles.

The specific surface area and pore size distribution studies were carried out for Ru-TiO_2-IL and Ru-TiO_2 catalysts, using Autosorb 1C -Quantachrome instrument.

The specific surface areas of pure Ru-TiO_2-IL and Ru-TiO_2 samples were are determined by nitrogen physisorption measurements **Table I**. The BET surface area of pure TiO_2 samples is found to be 1070 m^2/g. **Table I** confirmed the drop-in surface area while loading the Ru metal of TiO_2. Such change occurs due to the blocking of TiO_2 pores by ruthenium metal crystals.

Table I. Physiochemical analysis of Ru-TiO_2-IL and Ru-TiO_2 samples.

Entry	Ru loading (wt%)	BET surface area (m^2/g)	Total pore Volume (mL/g)	Average pore diameter (nm)
1	Ru-TiO_2	10.59	0.876	3.1
2	Ru-TiO_2-IL	10.45	0.941	2.9

CO chemisorption was performed for pure Ru-TiO_2-IL and Ru-TiO_2 samples using model ASAP 2020C V1.09 G an instrument. Before going to CO adsorption, all samples (weighed approximately 0.12 g) were pre-treated in He atmosphere for 30 min, and in O_2 atmosphere for 15 min, and then only samples were allowed to for 60 min in a (5.0%) H_2/Ar gas flow (50 mL/min), and in He gas flow (15 min at 400°C) in a reaction chamber. After successful completion of pre-treatment process, all the samples were cooled down to 50°C under He gas flow. CO pulse measurements were recorded using (5.0%) CO/He gas flow (50 mL/min). Finally, the surface concentration and dispersion of metallic Ru were obtained from the CO pulse analysis data. All the data were summarized in **Table II [27]**.

Table II. Results of CO chemisorption, dispersion, area and average crystallite size of Ru metal.

Samples	S_{Ru} (m^2/g catalyst)	CO_{irr} uptake (micromol/g)	Dispersion (%)	Particle size [a] (nm)	Particle size (nm)[b]
Ru-TiO_2	3.15	63	11	11.6	20 (±0.5)
Ru-TiO_2-IL	3.11	62	13.1	7.7	10(±0.5)

a - Calculated by CO chemisorption method; b. Calculated by TEM analysis

The FTIR analysis of TiO_2 with respect to Ru-TiO_2-IL and Ru-TiO_2 catalysts were carried out in the range of 400-4000cm^{-1} **Fig. 2**. In Ru loaded TiO_2, a clear peak of O-Ti-O bonding were found near 445 and 708cm^{-1}. The representing band for δ-H_2O bending appeared near to 1605cm^{-1}. A broad absorption band showing the-O and O-Ti-O flexion vibration band found between 400 cm^{-1} and 800 cm^{-1}. When metal ions are incapacitated to the exterior of TiO_2, the absorption band converts and instantaneously new adsorption bands developed. Upon adding of dopant, a small shift was noticed for the stretching vibration of Ti-O.

The XANES spectra at Ru K-edge of the Ru-TiO_2-IL and Ru-TiO_2 catalysts with respect to Ru foil were represented in the **Fig. 3**. The XANES spectrum of the Ru-TiO_2-IL catalyst was found similar to Ru foil, which indicates that the Ru species were reduced to the metallic sate, while XANES spectrum of Ru-TiO_2 catalyst was found much higher than the Ru foil, which represents that the Ru supported on TiO_2 remained in an oxidative state.

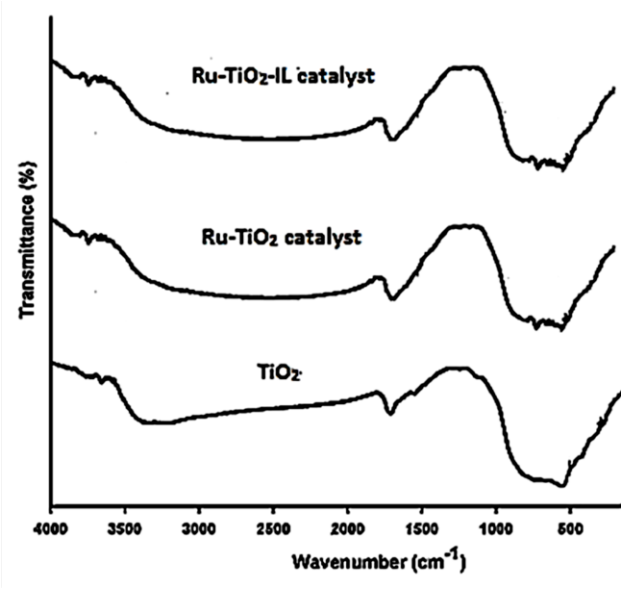

Fig. 2. Infrared data for Ruthenium metal doped Titanium dioxide nanoparticles.

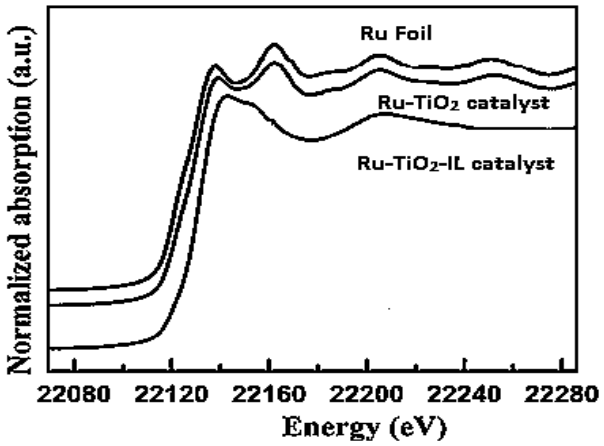

Fig. 3. XANES data for Ruthenium metal doped Titanium dioxide nanoparticles.

TEM micrographs of TiO_2, Ru-TiO_2-IL and Ru-TiO_2 are shown in **Fig. 4**. Electron microscopy reveals the morphology of the TiO_2, Ru-TiO_2-IL and Ru-TiO_2. It was clearly observed that for Ru-TiO_2 catalyst, many severely strained ruthenium nanoparticles larger than 25±5nm were found on the surface of TiO_2 while in Ru-TiO_2-IL catalysts, ultrafine Ru nanoparticles with uniform particle size were dispersed on the surface of TiO_2. It's worth noted here that no particles larger than 20 nm, observed despite our careful observation. More intuitively, the average particle size of the Ru-TiO_2 catalyst was found to be 20±0.5nm. However, it was only 10±0.5nm with narrower particle size spreading for the Ru-TiO_2-IL catalyst. These observations indicated that the reaction

medium type could remarkably affect the dispersion of Ru on theTiO_2 surface and ionic liquid to be an efficient reaction medium over conventional solvents to stabilize the smaller nano-sized particles of Ru. The catalyst loading on TiO_2 was calculated using inductively coupled plasma atomic emission spectrometer (ICP-AES, ARCOS from M/s. Spectro, Germany). 0.1 g of sample was digested in a minimum amount of conc. HNO_3 with heating, and volume made up to 10 ml. Theoretical (cation exchange capacity) and an experimental (ICP-AES) method was used to calculate the amount of Ru species in TiO_2. Both theoretical and experimental values were found to be in good agreement, and 2.5 wt% Ru was found in Ru-TiO_2-IL catalyst while in Ru-TiO_2 catalyst 2.1wt % Ru metal calculated. This protocol also minimizes the loss of Ru nanoparticles during the process.

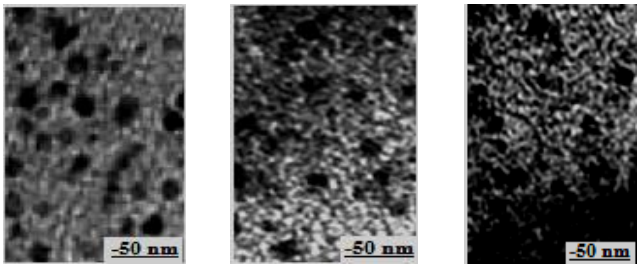

a. **Ru-TiO_2 catalyst** b. **Ru-TiO_2-IL catalyst** (Before catalyst) c. **Ru-TiO_2-IL catalyst** (After catalyst)

Fig. 4. TEM data for Ruthenium metal doped Titanium dioxide nanoparticles (a, b, c).

Hydrogenation of CO_2 was carried out using H_2 gas in the presence of both the catalysts (without any pretreatment) with functionalized ionic liquids separately at 80°C under high pressure reaction condition (**Scheme 1**). After the reaction, formic acid was isolated from the reaction mass followed by the nitrogen flow at 125-130°C. The results obtained while optimizing the reaction conditions with respect to TON/TOF value of formic acid were summarized in **Table III**, entry 1-17. Acid –Base titration using phenolphthalein indicator and 1H NMR analysis was used to calculate the quantity of formic acid formed after the hydrogenation reaction **[26]**. ^{1}HNMR analysis also confirmed no decomposition of formic acid as well as an ionic liquid during the experimental condition **[25]**.

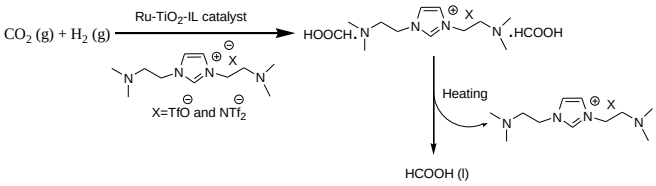

Scheme 1. Catalytic CO_2 hydrogenation and Formic acid isolation step.

Initially, both the catalysts were tested under same reaction condition for CO_2 hydrogenation and high TON/TOF value was obtained with [DAMI] [$CF_3CF_2CF_2CF_2SO_3$] immobilized Ru-TiO_2-IL (**Table III**, Entry 1 & 2). All the other important reaction parameters and technical variables were investigated using [DAMI] [$CF_3CF_2CF_2CF_2SO_3$] or [DAMI] [BF_4] immobilized Ru-TiO_2-IL (**Table III**, Entry 3-17). While optimizing the reaction temperature for hydrogenation reaction, we obtained good TON/TOF value at 100°C when, the total H_2/CO_2 gas pressure was 40 MPa (**Table III**, Entry 3). Effect of water was also studied on the reaction kinetics of CO_2 hydrogenation reaction only with 2 ml of water; we obtained the formic acid with a high TON/TOF value (**Table III**, entry 12) mainly because CO_2 may react with water and an amine group of ionic liquid to give offers bicarbonates which may act as a perfect substrate for the hydrogenation reaction. $RuCl_3$ was also evaluated to replace Ru-TiO_2 and Ru-TiO_2-IL catalytic system for the hydrogenation reaction, but formic acid was obtained with low TON/TOF value compared to [DAMI][$CF_3CF_2CF_2CF_2SO_3$] immobilized Ru-TiO_2-IL (**Table III**, Entry 17).

Table III. Hydrogenation of CO_2 to Formic acid using ionic liquid immobilized TiO_2 dropped Ru metal **[1]**.

Entry	Catalytic system	P (H_2) (P_{total}) (MPa) [2]	Temperature (°C)	Time (h)	TON[3]	TOF[4]
1.	Ru-TiO_2-IL /[DAMI][TfO]	20 (40)	80	2.5	630	252
2.	Ru-TiO_2/[DAMI][TfO]	20 (40)	80	2.5	555	222
3.	Ru-TiO_2-IL /[DAMI] [NTf_2]	20 (40)	80	2.5	615	246
4.	Ru-TiO_2-IL /[DAMI][TfO]	20 (40)	100	2.5	632.5	253
5.	Ru-TiO_2-IL /[DAMI][TfO]	20 (40)	120	2.5	632.5	253
6.	Ru-TiO_2-IL /[DAMI][TfO]	20 (40)	50	2.5	487.5	195
7.	Ru-TiO_2-IL /[DAMI][TfO]	20 (40)	100	3.5	532.4	152
8.	Ru-TiO_2-IL /[DAMI][TfO]	20 (40)	100	0.5	212.5	425
9.	Ru-TiO_2-IL /[DAMI][TfO]	10 (20)	100	2.5	487.5	195
10.	Ru-TiO_2-IL /[DAMI][TfO]	30 (60)	100	2.5	630.5	252
11.	Ru-TiO_2-IL /[DAMI][TfO]+ H_2O (1 mL)	20 (40)	100	2.5	645	258
12.	Ru-TiO_2-IL /[DAMI][TfO]+H_2O (2 mL)	20 (40)	100	2.5	675	270
13.	Ru-TiO_2-IL /[DAMI][TfO]+H_2O (3 mL)	20 (40)	100	2.5	679	272
14.	Ru-TiO_2-IL / [DAMI] [TfO] (0.100g)+ H_2O (2 mL)	20 (40)	100	2.5	679	272
15.	Ru-TiO_2-IL / [DAMI] [TfO] (0.500g)+ H_2O (2 mL)	20 (40)	100	2.5	680	272
16.	Ru-TiO_2-IL / [DAMI][NTf_2]+ H_2O (2 mL)	20 (40)	100	2.5	650.5	260
17.	$RuCl_3$ (0.07g)[4]+ [DAMI][NTf_2](0.250g)	20 (40)	100	2.5	560.5	224

After the reaction, formic acid was isolated with the aid of N_2 gas and the [DAMI][$CF_3CF_2CF_2CF_2SO_3$] ionic liquid immobilized Ru-TiO_2-IL went for a recycling test after washing with diethyl ether. [DAMI] [$CF_3CF_2CF_2CF_2SO_3$] ionic liquid immobilized Ru-TiO_2-IL were recycled up to 5 times with slight loss of their catalytic action mainly because of agglomeration of Ru NPs which was also confirmed by TEM analysis of Ru NPs **Fig. 5**. A significant increase, in the particle size of Ru NPs from 10 ± 0.5 nm to 30 ±0.5 nm (due to the agglomeration of Ru NPs) may cause a drop in the catalytic activity of Ru NPs during recyclability test. AAS analysis also confirmed the catalyst leaching during recycling runs as the metal catalyst is not covalently attached to support.

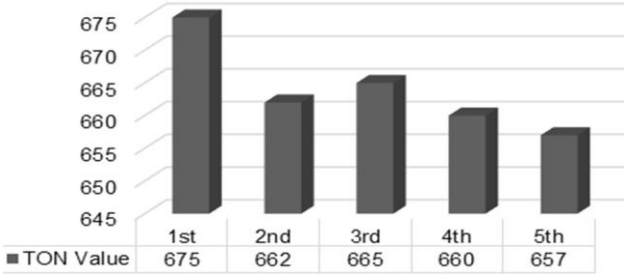

Fig. 5. Catalyst recycling experiment.

Conclusion

Here, we reported the synthesis of air/moisture stable, narrow size distributed TiO_2 supported Ru nanoparticles. Ru NPs in TiO_2 support. [DAMI][$CF_3CF_2CF_2CF_2SO_3$] ionic liquid immobilized Ru-TiO_2-IL catalyst was found highly active in terms of TON/TOF value of formic acid over conventional and Ru-TiO_2 catalyst. Effect of water was also studied during the CO_2 hydrogenation reaction. The presence of functionalized ionic liquid as well as water was promising. Five times catalyst recycling, low catalyst loading and selectivity were the major outcomes of this proposed protocol.

Acknowledgements

This work is financially supported by DST Fast Track (SB/FT/CS-124/2012), India.

References

1. Leunga, D. Y. C.; Caramannab, G. C.; Maroto-Valerb, M. M; *Renewable and Sustainable Energy Reviews*, **2014**, *38*, 426. **DOI:** 10.1016/j.rser.2014.07.093
2. Sreenivasulu, B.; Gayatri, D. V.; Sreedhar, I.; Raghavan, K. V; *Renewable and Sustainable Energy Reviews*, **2015**, *41*, 1324. **DOI:** 10.1016/j.rser.2014.09.029
3. Li, Y.; Chan, S. H.; Sun, Q; *Nanoscale*, **2015**, *7*, 8663. **DOI:** 10.1039/c5nr00092k
4. Najafabadi, A. T; *International Journal of Energy Research*, **2013**, *37*, 485. **DOI:** 10.1002/er.3021
5. Sankaranarayanan, S.; Srinivisana, K; *Indian journal of Chemistry*, **2012**, *51A*, 1252.
6. Styring, P.; Amstron, K; *Chimica Oggi-Chemistry Today*, **2011**, *29*, 34.
7. Ola, O.; Maroto-Valera, M. M.; Mackintosh, S; *Energy Procedia*, **2013**, *37*, 6704. **DOI:** 10.1016/j.egypro.2013.06.603
8. Miao, C-X.; Wang, J-Q.; He, L-N; *The Open Organic Chemistry Journal*, **2008**, *2*, 68. **DOI:** 10.2174/1874095200801020068
9. Aresta, M.; Dibenedetto, A; *J. Braz. Chem. Soc.* **2014**, *25*, 2215. **DOI:** 10.5935/0103-5053.20140257
10. Von der Assen, N.; Voll, P.; Peters, M.; Bardow, A; *Chem. Soc. Rev*. **2014**, *43*, 7982. **DOI:** 10.1039/c3cs60373c
11. Moret, S.; Dyson, P. J.; Laurenczy, G; *Nature Communications*, **2014**, *5*, 1. **DOI:** 10.1038/ncomms5017
12. Ghandi, K; *Green and Sustainable Chemistry*, 2014, *4*, 44. **DOI:** 10.4236/gsc.2014.41008
13. Ratti, R; *Advances in Chemistry*, **2014**, *2014*, 1. **DOI:** 10.1155/2014/729842
14. Duan, X.; Ma, J.; Lianc, J.; Zheng, W; *Cryst. Eng. Comm.* **2014**, *16*, 2550. **DOI:** 10.1039/c3ce41203b
15. Hayes, R.; Warr, G. G.; Atkin, R; *Chem. Rev*. **2015**, *115*, 6357. **DOI:** 10.1021/cr500411q
16. Richter, K.; Campbell, P. S.; Baecker, T.; Schimitzek, A.; Yaprak, D.; Mudring, A-V; *Physica status solidi (b)*, **2013**, *6*, 1152. **DOI:** 10.1002/pssb.201248547
17. Prechtl, M. H. G; Campbell, P. S; *Nanotechnology Reviews* **2013**, *2*, 577. **DOI:** 10.1515/ntrev-2013-0019
18. Zhang, B.; Yan, N; *Catalysts*, **2013**, *3*, 543. **DOI:** 10.3390/catal3020543
19. Vollmer, C.; Janiak, C; *Coord. Chem. Rev.* **2011**, *255*, 2039. **DOI:** 10.1016/j.ccr.2011.03.005
20. Neouze, M-A; *J. Mater. Sci.* **2010**, *20*, 9593. **DOI:** 10.1039/c0jm00616e
21. Scholten, J. D.; Leal, B. C.; Dupont, J; *ACS Catal.* **2012**, *2*, 184. **DOI:** 10.1021/cs200525e
22. Yan, N.; Xiao, C.; Kou, Y; *Coord. Chem. Rev.* **2010**, *254*, 1179. **DOI:** 10.1016/j.ccr.2010.02.015
23. Prechtl, M. H. G.; Campbell, P. S.; Scholten, J. D.; Fraser, G. B.; Machado, G.; Santini, C. C.; Dupont, J.; Chauvin, Y; *Nanoscale*, **2010**, *2*, 2601. **DOI:** 10.1039/c0nr00574f
24. Dupont, J.; Scholten, J. D; *Chem. Soc. Rev.* **2010**, *39*, 1780. **DOI:** 10.1039/b822551f
25. Srivastava, V; *Catalysis Letters*, **2014**, *144*, 1745. **DOI:** 10.1007/s10562-014-1321-6
26. Hamzaha, N.; Nordinc, N. M.; Nadzri, A. H. A.; Nik, Y. A.; Kassim, M. B.; Yarmo, M. A; *Applied Catalysis A: General*, **2012**, *419-420*, 133. **DOI:** 10.1016/j.apcata.2012.01.020
27. Kumar, V. P.; Harikrishna, Y.; Nagaraju, N.; Chary, K. V. R; *Indian Journal of Chemistry*, **2014**, *53A*, 516.

